Ultra-narrow optical hole burning in ruby
Szabo, Alex

Publisher’s version / Version de l'éditeur:
https://doi.org/10.1016/0022-2313(93)90052-O
Journal of Luminescence, 56, 1-6, pp. 47-50, 1993-10

Ultra-narrow Optical Hole Burning in Ruby

Alex Szabo
Institute for Microstructural Sciences
National Research Council of Canada
Ottawa, Ontario, K1A 0R6, Canada

Abstract

By applying a large magnetic field (~ 3.5T) along the crystal axis, the homogeneous linewidth of the $^4A_2(-1/2)\rightarrow\bar{E}(-1/2)$ optical transition of Cr^{3+} in dilute ruby is narrowed due to a suppression of Cr-Cr electron spin flipping. A holewidth as narrow as 17.9 kHz (FWHM) is observed using a pump-probe technique. In contrast to earlier low field results which gave strictly Lorentzian lineshapes, the high field lineshape is Gaussian. Arguments are presented that suggest the lineshape is determined by coherence rather than by dissipative effects. Achievement of the latter limit will require improvements in the long term frequency stability of the laser and an increase in sensitivity to allow pump-probe observations at low Rabi frequencies (< 5 kHz).

1. Introduction

Optical hole-burning (HB) of inhomogeneously broadened transitions in solids has been a subject of recent interest both for technological and scientific reasons. The application of HB for digital (frequency [1] and time domain [2]) and analog [3,4] information storage and processing [5] is receiving increased attention [6]. In part, this activity has prompted a closer look at the fundamental origins of the optical dephasing time T_2 of impurity atoms and molecules in solids [7-11]. T_2 is important for information storage since it is the ratio of inhomogeneous to homogeneous width ($1/\pi T_2$) that determines the storage capacity [1]. Dephasing has, of course, long been studied in magnetic resonance [12] which is serving as a rich source of insights and knowledge for understanding optical dephasing.

For ionically doped solids, nuclear [9] and electron [11,13] spin flipping have been shown to ultimately determine both optical and magnetic [12] dephasing at low temperatures. The role of host nuclear spin flipping has been directly demonstrated by magic angle pumping of the host F nuclei in Pr^{3+}:LaF_3 and observation [14,15] of a lengthening of the D_1 transition dephasing time. Electron spin flipping effects on the $^4A_2(-1/2)\rightarrow\bar{E}(-1/2)$ (hereafter $R_1(-1/2)$ etc.) transition in ruby have been directly demonstrated using R_2 optical pumping [13]. More recently [16], the suppression of electron spin flipping at high magnetic fields has been studied using photon echoes for the R_1 (-3/2) transition in ruby. The latter results suggest the attainment of the "superhyperfine limit" in which T_2 is determined only by flipping of distant host lattice Al nuclear spins and frozen core [12,17] Al spins surrounding the Cr^{3+} electronic spin. In this paper we extend earlier homogeneous linewidth studies [18] at low fields (~ 4 kG) to high fields (~ 35 kG) using both frequency (HB) and time domain (free induction decay (FID)) techniques for the R_1(-1/2) transition in dilute ruby. It should be noted that the R_1(-1/2) transition differs from R_1(-3/2) in two important respects. (1) The ground frozen core for S = -3/2 is much larger [19] (~ 400 Al) than for S = -1/2 (~ 13 Al) and (2) the R_1(-1/2) transition more closely approaches an ideal two state inhomogeneously broadened system. Since R_1(-1/2) has the same spin value in ground and excited states, the effect of spin mixing is minimized and the optical transition proceeds essentially without accompanying Al nuclear flips.

2. Experiment

A pump-probe technique described earlier [18] was used to study HB in dilute (0.0034 Wt% Cr_2O_3 = 0.0023 at.%) ruby. A major requirement for these high resolution experiments was an ultra-narrow (< 2 kHz peak to peak) dye laser linewidth to allow observation of HB widths of ~ 20 kHz. This was achieved using a frequency modulation technique [20]. Pump and probe pulsewidths were 50- 100 μsec and separated by 10 μsec. The probe power was 1-5 % of that of the pump. A frequency synthesizer-amplifier combination was used to drive an acousto-optic (AO) modulator to provide precise tuning of the probe. The AO pump pulse frequency was determined by a fixed crystal controlled oscillator. All experiments were done with a sample temperature of 2 K and in a magnetic field supplied by a split-coil, high homogeneity superconducting magnet.

3. Results

Fig. 1 shows the holeshape measured for the R(-1/2) line at a field of ~ 35 kG parallel to the c axis. Regression analysis shows that the lineshape is best fit by a Gaussian rather than the Lorenztian shape observed earlier [18] at low fields (the Gaussian residual is ~ 3× smaller than the Lorenztian). A FID intensity decay is shown in Fig. 2. Because of the low Rabi frequency and the reduced population in the $^4A_2(-1/2)$ level at high fields, the signal is weak and only about one order of decay could be measured. Over this range the decay looks exponential with a decay time T_d = 10.2 μsec which, in the standard optical Bloch theory, implies a $T_2 > 4\ T_d$ = 40.8 μsec. A summary of observed holewidths and shapes for various Rabi frequency-pulse width combinations is given in Table 1 along with holewidth calculations [21] using a plane-wave Gauss-Markov [10] model of modified optical Bloch equations (OBE). The rationale for this choice of model is the observed [20] failure of the standard OBE in describing the power dependence of optical HB in ruby. For the calculations, a value T_2 = 41 μsec was used as a lower limit obtained from the FID data of Fig. 2. Also we assumed a correlation time $\tau_c = T_2$ as in ref. 20.

4. Discussion

Referring to Fig. 1 and Table 1, the $R_1(-1/2)$ hole widths are seen to be smaller (by ~ 2×) than those obtained at low fields [18]. At low fields, the $R_1(-1/2)$ homogeneous linewidth for a dilute 0.0023 at.% ruby has been shown [18] to be still dominated by the magnetic field fluctuations produced by Cr-Cr spin flips. Increasing the field to 35 kG eliminates, to a large extent, Cr spin flipping effects since most (~ 93%) of the Cr ions are in the ground spin state ($^4A_2(-3/2)$) at 2 K. This leaves Al nuclear spins of the host lattice as the only dephasing source, aside from radiative lifetime effects. Another striking aspect of the high field data is the Gaussian lineshapes observed for a 50 μsec burn time and a Rabi frequency $\chi/2\pi$ in the range 5.8 to 11.0 kHz (i.e. pulse angles $\leq \pi$). While we had earlier speculated [22] that the Gaussian lineshape was consistent with a spectral diffusion model suggested by the photon echo studies of ref. 16, we now believe that the lineshape and width are primarily determined by coherence effects and the finite pump-probe widths. This idea is supported by the theoretical lineshape shown in Fig. 3 which closely approximates a Gaussian. Also the calculated Voight linewidths in Table 1 obtained by convoluting the (Gaussian) burn and (Lorentzian) probe widths are, within experimental error, in good agreement with experimental values. If the normal OBE are used, we obtain for a 50 μsec burn time, a pump width [23] of 21.5 kHz (FWHM) essentially independent of Rabi frequency in the range 5.8 to 11.0 kHz. This convolutes with a Lorentzian probe width of 21.6 kHz to give a Voight width of 35.3 kHz - in clear violation of the experimental data.

Numerical studies of the Gauss-Markov OBE show that in order to obtain a linewidth solely determined by dissipation processes, (1) the burn time should be several times longer than T_2 and (2) the burn power must be low enough so that the pulse angle is much smaller than π over a time T_2, i.e. $\chi T_2 << \pi$. Accordingly the burn time was extended to 100 μsec (Table 1). Now we note that the calculated probe width of 6.4 kHz is mostly determined by T_2 rather than by the pulse width. However only a ~ 10% reduction of the hole width to 19.6 kHz was observed for

$\chi/2\pi = 4.8$ kHz. For larger χ, the pulse angles exceed π and theoretical lineshapes of the Bloch vector $w(\Delta)$ start to show nutation structure [21,24]. Such structure is not seen experimentally, possibly because (1) it is smoothed out when the probe lineshape is convoluted with the pump shape, and (2) variation of χ over the beam cross section. Longer burn times did not result in narrower linewidths, however power broadening may have still been present since sensitivity considerations limited the Rabi frequency to a minimum value of ~ 5 kHz. Also another parameter that may have affected the results is the long term stability of the laser which becomes a factor for burn times $\gtrsim$ 500 μsec (possibly as short as 300 μsec). Further work on the laser stability and sensitivity of hole detection is underway to clarify if the hole widths observed in this paper are dissipation limited.

Acknowledgment

The author thanks J. Froemel for technical assistance in this work.

Table 1

Experimental and theorectical linewidths (FWHM) for 0.0023 at% ruby at 2 K for a field of 35 kG along the c axis.

(a) Pump pulse width = 50 μsec

Experimental[a]			Theoretical[b]		
Burn Time (μsec)	Rabi Frequency (kHz)	Hole Width (kHz)	Voight Convoluted Width (kHz)	Pump Width (kHz)	Probe Width (kHz)
50	5.8	25.3(G)	19.9	13.7(G)	10.1(L)
50	8.2	25.7(G)	20.8	14.8(G)	10.1(L)
50	11.0	22.9(G)	21.8	15.5(G)	10.1(L)

(b) Pump pulse width = 100 μsec.

100	4.8	19.6[c](G)	13.0	9.1(G)	6.4(L)
100	8.2	28.0(-)	-	33.4[d]	6.4(L)
100	11.3	26.1(-)	-	30.7[d]	6.4(L)

a Hole widths are average of 4-6 runs. Typical spread of widths is ±2 kHz.

b Plane wave Gauss-Markov model with $T_2 = 41$ μsec = τ_c.

(L) = Lorenztian lineshape, (G) = Gaussian; (-) neither G nor L.

c Narrowest width observed = 17.9 kHz.

d Pump pulse angle exceeds π and theoretical lineshape shows nutation structure. Widths defined as in ref. 24.

References

1. A. Szabo, U.S. Patent No. 3,896,420 (1975). G. Castro, D. Haarer, R.M. Macfarlane and H.P. Trommsdorf, U.S. Patent No. 4,101,976 (1978).
2. T.W. Mossberg, Opt. Lett. 7(1982)77. ibid U.S. Patent No. 4,459,682 (1984). See also M.A. Friedlander and S. Meth, U.S. Patent No. 4,479,199 (1984).
3. A. Szabo, U.S. Patent No. 4,432,071 (1984).
4. A. Renn, A.J. Meixer and U.P. Wild, J. Chem. Phys. 92 (1990) 2748.
5. A. Renn, A.J. Meixer and U.P. Wild, J. Chem. Phys. 93 (1990) 2279. U.P. Wild and A. Renn, J. Mol. Elect. 7 (1991) 1.
6. Persistent Spectral Hole-Burning: Science and Applications, ed. W.E. Moerner (Springer-Verlag, Berlin 1988).
7. I.D. Abella, M.A. Kurnitt and S.R. Hartmann, Phys. Rev. 141 (1966) 391.
8. L.Q. Lambert, A. Compaan and I.D. Abella, Phys. Lett. 30A (1969) 153.
9. R.G. DeVoe, A. Wokaun, S.C. Rand and R.G. Brewer, Phys. Rev. B23 (1982) 3125.
10. P.R. Berman and R.G. Brewer, Phys. Rev. A32 (1985) 2784.
11. A. Szabo, T. Muramoto and R. Kaarli, Phys. Rev. B42 (1990) 7769.
12. W.B. Mims, Electron Paramagnetic Resonance, ed. S. Geschwind (Plenum, New York, 1972) p.263.
13. A. Szabo and J. Heber, Phys. Rev. A29 (1984) 3452.
14. S.C. Rand, A. Wokaun, R.G. DeVoe and R.G. Brewer, Phys. Rev. Lett. 43 (1979) 1868.
15. R.M. Macfarlane and R.M. Shelby, Opt. Lett. 6 (1981) 96.
16. J. Ganem, Y.P. Wang, D. Boye, R.S. Meltzer, W.M. Yen, R. Wannemacher and R.M. Macfarlane, Phys. Rev. Lett. 66 (1991) 695.
17. A. Szabo, Opt. Lett. 8 (1983) 486.
18. A. Szabo and R. Kaarli, Phys. Rev. B44 (1991) 12307.
19. A. Szabo, J. Opt. Soc. Am. B3 (1986) 514.
20. A. Szabo and T. Muramoto, Phys. Rev. A39 (1989) 3992.

21. A. Szabo and T. Muramoto, Phys. Rev. A37 (1988) 4040.

22. A. Szabo, Bull. Am. Phys. Soc. 36 (1991) 1943.

23. The hole actually narrows as the Rabi frequency is increased (up to a certain point) as discussed in ref. 24.

24. S. Huang, S. Quan, W. Qin and J. Yu, J. Lumin. 53 (1992) 231.

Figures

1. Hole shape seen in 0.0023 at% ruby for the $^4A_2(-1/2) \rightarrow \bar{E}(-1/2)$ optical transition at 693 nm. Field is ~ 35 kG along the crystal axis, temperature = 2.0 K. Regression analysis gives a 3× lower residual for Gaussian than for Lorenztian shape.
2. Hole shape calculated from Gauss-Markov modified optical Bloch equations. The population term w of the Bloch vector is plotted vs frequency showing an approximate Gaussian lineshape. Pulse width = 50 μsec and Rabi frequency = 11.0 kHz.
3. Free induction intensity decay in ruby for the parameters given in Fig. 1. A 1/e decay time of 10.2 μsec is obtained for a Rabi frequency of 10.5 kHz and pulse preparation time of 50 μsec.

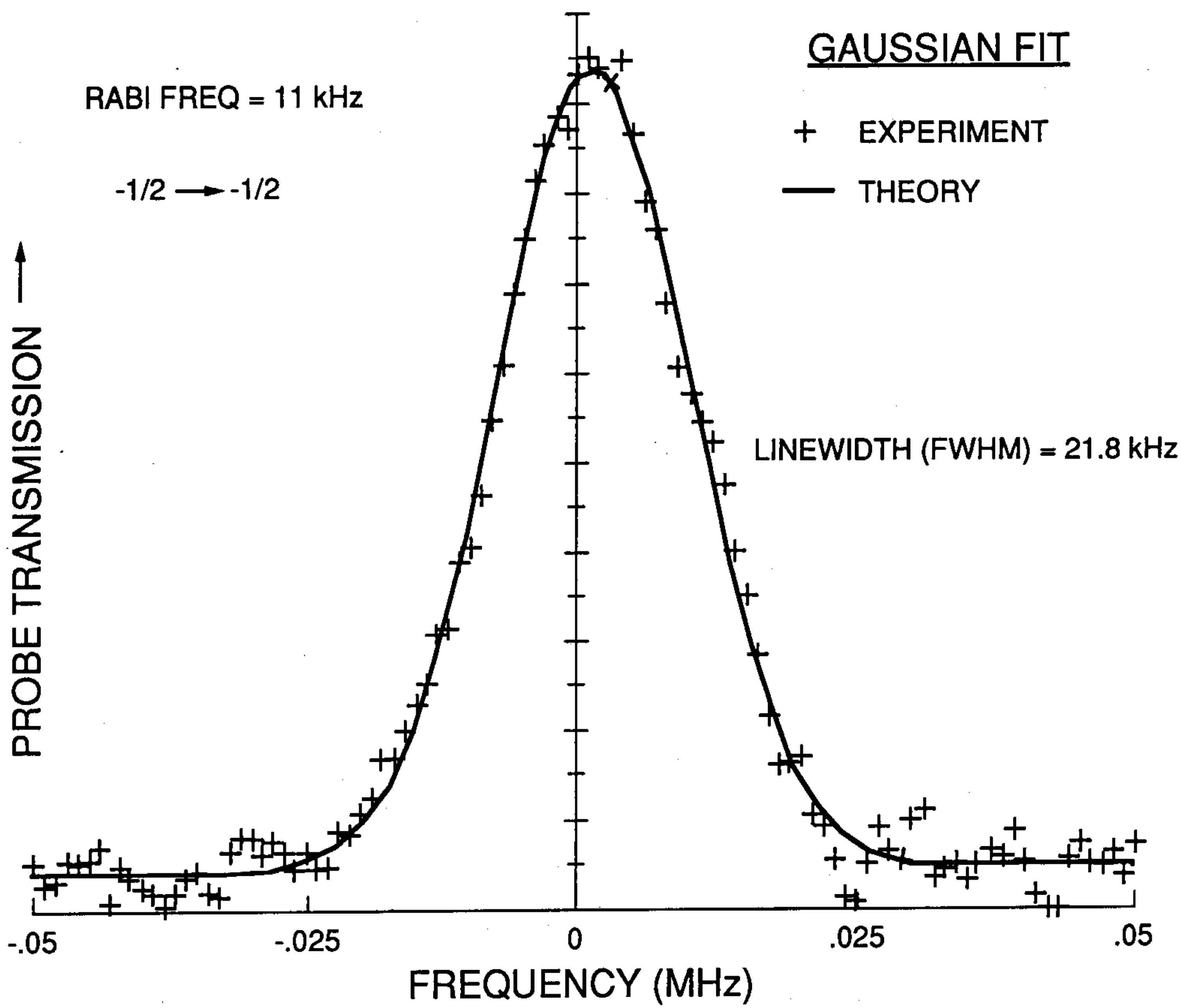
GAUSSIAN FIT
RABI FREQ = 11 kHz
-1/2 → -1/2
+ EXPERIMENT
— THEORY
LINEWIDTH (FWHM) = 21.8 kHz
PROBE TRANSMISSION
-.05
-.025
0
.025
.05
FREQUENCY (MHz)

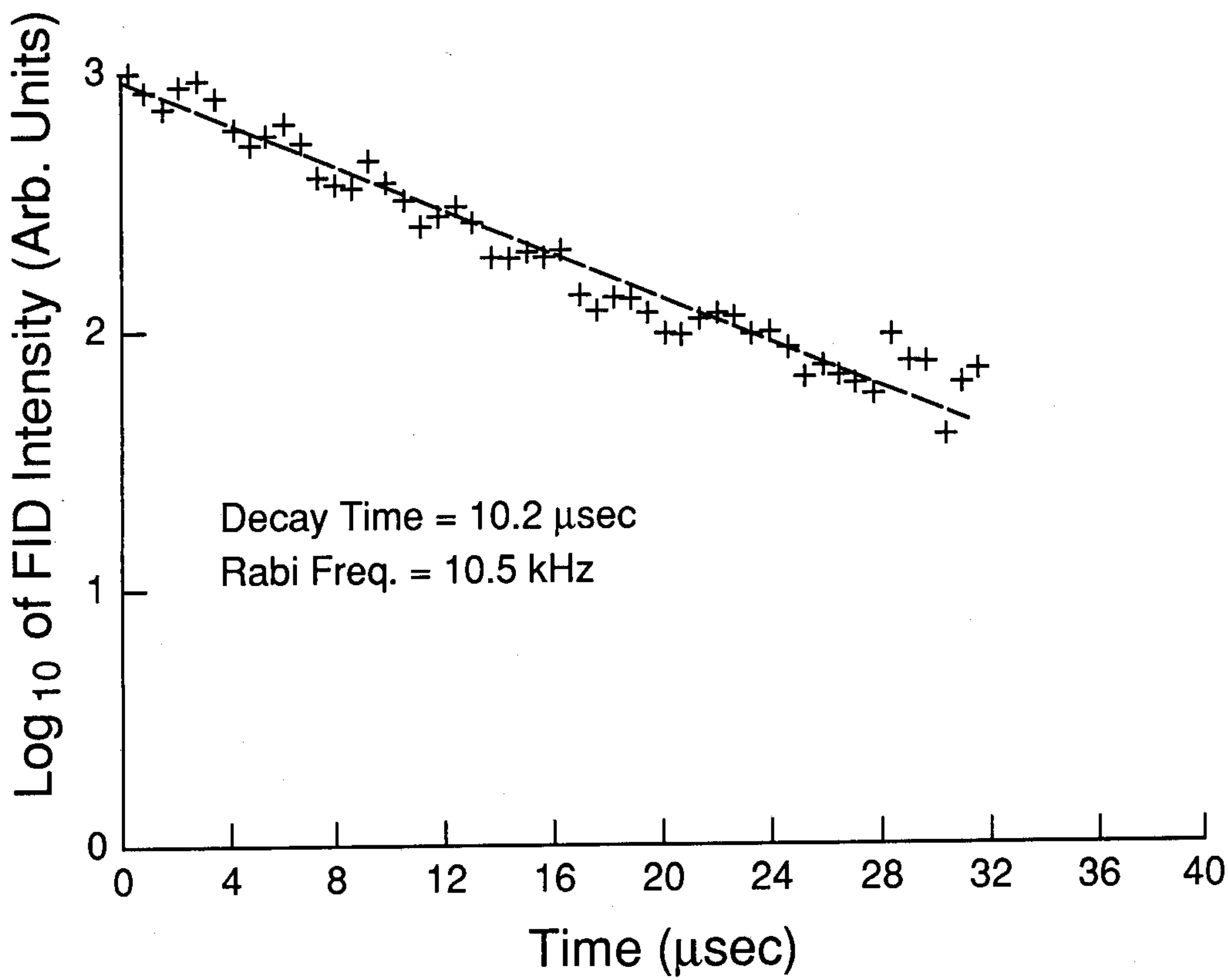
Log 10 of FID Intensity (Arb. Units)
3
2
1
0
0
4
8
12
16
20
24
28
32
36
40
Time (µsec)
Decay Time = 10.2 µsec
Rabi Freq. = 10.5 kHz

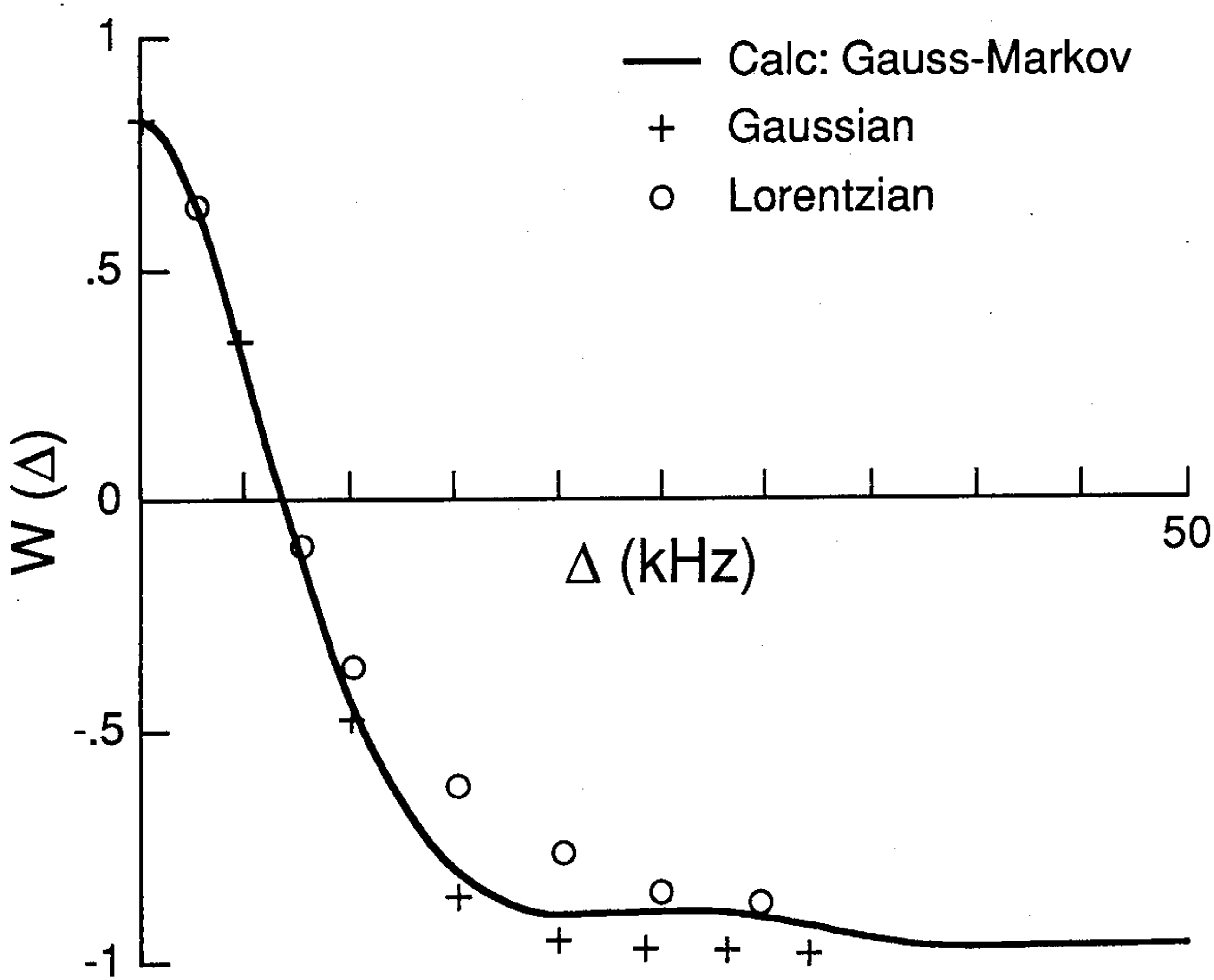
Calc: Gauss-Markov
Gaussian
Lorentzian
W (Δ)
Δ (kHz)
1
.5
0
-.5
-1
50